Research Article | Vol. 24, No. 25 | 12 Dec 2016 | OPTICS EXPRESS 28958

Optics EXPRESS

2*f*-wavelength modulation Fabry-Perot photothermal interferometry

JOHANNES P. WACLAWEK,* VOLKER C. BAUER, HARALD MOSER, AND BERNHARD LENDL

Institute of Chemical Technologies and Analytics, Vienna University of Technology, Getreidemarkt 9/164, 1060 Vienna, Austria
*johannes.waclawek@tuwien.ac.at

Abstract: Trace gas detection was performed by the principle of photothermal interferometry using a Fabry-Perot interferometer combined with wavelength modulation and second harmonic detection. The sensor employed a compact, low-volume gas cell in an overall robust set-up without the use of any moveable part. A quantum cascade laser was used as powerful mid-infrared excitation source to induce refractive index changes in the sample, whereas a near-infrared laser diode served as probe source to monitor the photo-induced variations. The functional principle of the selective sensor was investigated by detection of sulfur dioxide. For the targeted absorption band centered at 1379.78 cm^{-1} a 1 σ minimum detection limit of about 1 parts per million by volume was achieved. The work demonstrates high potential for further sensor miniaturization down to a sample volume of only a few mm^3. Limitations and possible improvements of the sensor regarding sensitivity are discussed.

OCIS codes: (120.2230) Fabry-Perot; (120.3180) Interferometry; (140.5965) Semiconductor lasers, quantum cascade; (300.6340) Spectroscopy, infrared; (300.6430) Spectroscopy, photothermal.

References and links

1. S. E. Bialkowski, *Photothermal Spectroscopy Methods for Chemical Analysis* (John Wiley & Sons, 1996).
2. A. Miklós, P. Hess, and Z. Bozóki, "Application of acoustic resonators in photoacoustic trace gas analysis and metrology," Rev. Sci. Instrum. **72**(4), 1937 (2001).
3. C. C. Davis and S. J. Petuchowski, "Phase fluctuation optical heterodyne spectroscopy of gases," Appl. Opt. **20**(14), 2539–2554 (1981).
4. W. Jin, Y. Cao, F. Yang, and H. L. Ho, "Ultra-sensitive all-fibre photothermal spectroscopy with large dynamic range," Nat. Commun. **6**, 6767 (2015).
5. J. Stone, "Measurements of the Absorption of Light in Low-Loss Liquids," J. Opt. Soc. Am. **62**(3), 327–333 (1972).
6. D. L. Mazzoni and C. C. Davis, "Trace detection of hydrazines by optical homodyne interferometry," Appl. Opt. **30**(7), 756–764 (1991).
7. A. J. Campillo, S. J. Petuchowski, C. C. Davis, and H.-B. Lin, "Fabry-Perot photothermal trace detection," Appl. Phys. Lett. **41**(4), 327–329 (1982).
8. B. C. Yip and E. S. Yeung, "Wavelength modulated Fabry-Perot interferometry for quantitation of trace gas components," Anal. Chim. Acta **169**, 385–389 (1985).
9. F. Yang, Y. Tan, W. Jin, Y. Lin, Y. Qi, and H. L. Ho, "Hollow-core fiber Fabry-Perot photothermal gas sensor," Opt. Lett. **41**(13), 3025–3028 (2016).
10. G. A. Reider, *Photonics – An Introduction* (Springer, 2016), Chap. 4.
11. P. Werle, "A review of recent advantages in semiconductor laser based gas monitors," Spectrochim. Acta A **54**(2), 197–236 (1998).
12. J. Hodgkinson and R. P. Tatam, "Optical gas sensing: a review," Meas. Sci. Technol. **24**(1), 012004 (2013).
13. S. Schilt and L. Thévenaz, "Wavelength modulation photoacoustic spectroscopy: Theoretical description and experimental results," Infrared Phys. Technol. **48**(2), 154–162 (2006).
14. P. Patimisco, G. Scamarcio, F. K. Tittel, and V. Spagnolo, "Quartz-Enhanced Photoacoustic Spectroscopy: A Review," Sensors (Basel) **14**(4), 6165–6206 (2014).
15. F. K. Tittel, D. Richter, and A. Fried, "Mid-Infrared Laser Applications in Spectroscopy," in *Solid-State Mid-Infrared Laser Sources*, I. T. Sorokina, K. L. Vodopyanov (Springer, 2003).
16. L. S. Rothman, I. E. Gordon, Y. Babikov, A. Barbe, D. C. Benner, P. F. Bernath, M. Birk, L. Bizzocchi, V. Boudon, L. R. Brown, A. Campargue, K. Chance, E. A. Cohen, L. H. Coudert, V. M. Devi, B. J. Drouin, A. Fayt, J.-M. Flaud, R. R. Gamache, J. J. Harrison, J. M. Hartmann, C. Hill, J. T. Hodges, D. Jacquemart, A. Jolly, J. Lamouroux, R. J. Le Roy, G. Li, D. A. Long, O. M. Lyulin, C. J. Mackie, S. T. Massie, S. Mikhailenko, H. S.

#274314 http://dx.doi.org/10.1364/OE.24.028957
Journal © 2016 Received 23 Aug 2016; revised 28 Nov 2016; accepted 29 Nov 2016; published 7 Dec 2016

Optics EXPRESS

P. Müller, O. V. Naumenko, A. V. Nikitin, J. Orphal, V. Perevalov, A. Perrin, E. R. Polovtseva, C. Richard, M. A. H. Smith, E. Starikova, K. Sung, S. Tashkun, J. Tennyson, G. C. Toon, V. G. Tyuterev, G. Wagner, "The HITRAN2012 molecular spectroscopic database," J. Quant. Spectrosc. Radiat. Transf. **130**, 4–50 (2013).
17. J. P. Waclawek, R. Lewicki, H. Moser, M. Brandstetter, F. K. Tittel, and B. Lendl, "Quartz-enhanced photoacoustic spectroscopy-based sensor system for sulfur dioxide detection using a CW DFB-QCL," Appl. Phys. B **117**(1), 113–120 (2014).
18. B. Fischer, "Optical microphone hears ultrasound," Nat. Photonics **10**(6), 356–358 (2016).
19. Y. Tan, C. Zhang, W. Jin, F. Yang, H. L. Ho, and J. Ma, "Optical fiber photoacoustic gas sensor with graphene nano-mechanical resonator as the acoustic detector," IEEE J. Sel. Top. Quantum Electron. **23**, 5600211 (2016).
20. P. L. Meyer and M. W. Sigrist, "Atmospheric pollution monitoring using CO_2 laser photoacoustic spectroscopy and other techniques," Rev. Sci. Instrum. **61**(7), 1779 (1990).

1. Introduction

The absorption of light by molecules causes an excitation of internal energy levels, which in turn may lead to sample heating by energy transfer due to collisional relaxation. A change in temperature causes in turn a change in pressure and density, affecting the refractive index of the sample. Changes of thermodynamic properties are used for trace detection in photothermal spectroscopy (PTS) and photoacoustic spectroscopy (PAS). PTS methods typically monitor a change in the refractive index of the sample [1], whereas PAS techniques detect acoustic waves. The absorption of modulated light causes transient changes of the sample properties. By this means two waves are simultaneously generated: A heavily damped thermal wave with a wavelength in the sub-mm range and a slightly damped acoustic wave with a wavelength in the cm range [2]. Due to different damping coefficients and wavelengths the two waves are spatially separated and can be investigated independently. In contrast to classical transmission spectroscopy, where according to the Beer-Lambert law sensitivity is enhanced with pathlength, PTS is classified as an indirect method for optical absorption analysis, which measures the effect that optical absorption induces in the sample. PTS signals are generally proportional to the temperature change in a sample. A photo-induced temperature change within the excited sample volume is directly proportional to the concentration and absorption coefficient of the absorbing molecule as well as to the laser power, and inversely proportional to the modulation frequency and cross-section of the laser beam. Hence, with a given laser power higher temperature changes can be induced in smaller excitation volumes, offering the possibility for sensor miniaturization. Therefore, PTS signal generation will greatly benefit from high power laser excitation and ultra-low volume sample cells.

Typical PTS setups employ an excitation laser to heat the sample and a probe laser to monitor refractive index changes resulting from heating. The change in refractive index causes a phase shift of light passing through the heated sample, which can be measured with high sensitivity using an interferometer. Several interferometer types, such as Mach-Zehnder [3,4], Jamin [5,6], or Fabry-Perot [7–9] setting have been applied to measure a temperature induced phase shift of light. In single-pass interferometers (as Mach-Zehnder and Jamin) the probe beam is split into two beams, whereas one beam is transmitted through the heated sample region prior recombination with the other beam, which remains unaffected forming the reference. The transmitted optical power by the interfering beams depend on the relative phase of the individual beams, offering the possibility to measure small changes in the refractive index [10]. A different type of interferometer is the Fabry-Perot interferometer (FPI), which uses an optical cavity for multi-wave interference instead of a single-pass design. The FPI consists of two parallel aligned, partially transmitting mirrors in which a beam undergoes multiple reflections. Changes in the refractive index can be measured easily by detection of the transmitted intensity through the FPI, which is again dependent on the relative phase of the interfering waves.

The generation and detection of PTS signals requires transient heating of the sample gas. This may be performed by wavelength modulation spectroscopy (WMS) where the emission frequency of a tunable laser is periodically modulated and the transducer signal is detected by

Optics EXPRESS

a lock-in amplifier at a harmonic of the modulation frequency [11]. Wavelength modulation (WM) and second harmonic (2*f*) detection in particular is a very powerful method to increase the signal to noise ratio (SNR), as well as the selectivity of a given measurement. This scheme has been used for detection of trace gases in direct and indirect spectroscopic methods [11–14]. Detection of the second harmonic components yield signals, which are roughly proportional to the second derivative of the absorption spectrum. A significant improvement of the SNR employing 2*f*-WMS results because on the one hand the detection within a narrow frequency interval is shifted to a higher frequency where 1/*f* noise is reduced, and on the other hand because 2*f*-WMS is sensitive to the spectral shape or curvature of the absorption line rather than to absolute absorption levels [11,12]. The lineshape of a molecular absorption strongly depends on the gas pressure. At atmospheric pressure lineshapes are broadened due to molecular collisions. The reduction of the sample pressure will decrease pressure broadened linewidths which in turn will increase the curvature of the lineshapes and thus sensitivity. Furthermore, the 2*f*-WM scheme eliminates efficiently linear slopes of spectra. By this means any background absorptions originating from broad featureless bands, such as undesired absorptions caused from cell components (e.g. windows) are efficiently suppressed [15]. Only non-linear absorption features lead to signals that have components which are periodic with the modulation frequency and its higher harmonics. Thus, 2*f*-WMS is a zero-background technique. Furthermore, the selectivity of a given measurement is greatly improved when absorption lines are resolved from other interfering lines by pressure reduction in the case of multi-gas samples, as well as by suppression of signals from broad featureless absorptions, such as pressure-broadened bands of large molecules.

The presented work reports on the new combination of Fabry-Perot photothermal interferometry (FP-PTI) together with WM and second harmonic detection (2*f*-WM) using a simple absorption cell and semiconductor lasers in transverse configuration. This arrangement enables the construction of robust and compact trace gas sensors without the use of any moveable part. The spacing between the mirrors of the used FPI was fixed to a distance of 1 mm, yielding an ultra-low volume gas cell with a total volume of < 0.7 cm^3. Such a low cell volume entails a fast sensor response time and low sample diversion. The FP-PTI cell can be operated in a wide range of temperatures, in principle being limited by the material characteristics of the employed optics and the cell body, which may exceed 1000 K. Moreover, the presented setup exhibits a very high potential for further miniaturization even down to the point of micro-electro-optical-system (MEOS) integration on a chip. Refractive index changes induced by an excitation laser were monitored by a probe laser intersecting the excitation beam. High sensitivity was accomplished by employing a small interferometer spacing together with the use of a continuous wave (CW) distributed feedback (DFB) quantum cascade laser (QCL) as excitation source. Thus, strong fundamental absorption features of sample molecule in the mid-infrared (mid-IR) region could be targeted along with high laser power. Selectivity is achieved by employing 2*f*-WM and second harmonic detection at reduced sample pressure. The WM could be easily implemented by modulating the injection current of the excitation laser. Detection of refractive index changes were performed by a CW-DFB laser diode (LD) emitting in the vicinity of 1600 nm together with a photodiode. This near-infrared region offers matured technology where reasonable optical components are available. The metrological qualities of the 2*f*-WM FP-PTI detection principle was investigated using sulfur dioxide (SO_2) as target molecule.

2. Sensor operation principle and system architecture

2.1 Sensor operation principle

The refractive index change of a sample is directly proportional to the temperature change connected by the thermo-optic coefficient (d*n*/d*T*), which is linear over a narrow temperature range for most samples. The change in the refractive index primarily depends on a change in

Optics EXPRESS

density. In general the density decreases with temperature and therefore the refractive index becomes lower by sample heating. In case of a small refractive index variation, the total refractive index n of the sample is given by [1]

$$n = n_0 + \Delta n = n_0 + \left(\frac{dn}{dT}\right)\Delta T, \tag{1}$$

where n_0 is the refractive index of the sample in thermal equilibrium, Δn is the refractive index change and ΔT is the temperature change due to photothermal heating. A change of the refractive index can be measured by the phase shift of light passing through a Fabry-Perot interferometer (FPI). Light incident on the input mirror is partially transmitted into the interferometer and then partially reflected between the mirrors, forming an infinite series of partial waves in the forward and backward direction, respectively. An optical wave fulfilling the resonance condition, i.e. the spacing of the two mirrors corresponds to a multiple of the wavelength, is transmitted through the resonator. The transmitted intensity I_T through the FPI is given by [10]

$$I_T = I_0 \frac{1}{1+\left(\frac{2F}{\pi}\right)^2 \sin^2\left(\frac{\Delta\varphi}{2}\right)}, \tag{2}$$

where I_0 is the incident intensity, $\Delta\varphi$ is the phase difference and F is the finesse of the optical cavity, which is only determined by the reflectivity R of the mirrors:

$$F = \pi \frac{\sqrt{R}}{1-R}. \tag{3}$$

The phase difference for a cavity round trip, which is twice the distance d of the FPI, is given by

$$\Delta\varphi = \frac{2\pi}{\lambda_0} 2nd\cos\theta, \tag{4}$$

where λ_0 is the vacuum wavelength and cos θ is the angle of incidence. According to Eq. (4) a variation of n will cause a variation of $\Delta\varphi$ and can therefore be easily measured by detection of the transmitted laser intensity through the FPI incorporating the sample. Figure 1 illustrates the sensor operation principle; the periodic transmission function [Eq. (2)] of an optical cavity is shifted with respect to the vacuum wavelength when the refractive index of a sample in between the mirrors changes due to heating. This shift is monitored by a probe laser with fixed frequency as a change of transmitted intensity through the FPI. Highest sensitivity to variations in the phase difference is given in the vicinity of the inflection point of the periodic transmission function, which is near 75% transmission through the FPI. At this point the slope of the function is maximum and roughly linear over a narrow range. The slope of the transmission function and thus the detectable signal is directly proportional to the finesse of the cavity. Therefore, the sensitivity of the FPI based sensor can be simply adjusted by the reflectivity of the mirrors, which is an outstanding property compared to single-pass interferometers. However, enhancement of sensitivity by an increase of the reflectivity is only true to the extent that the source of limiting noise is not similarly enhanced. Limiting noise sources may be introduced by phase and intensity noise of the probe laser source, as well as mechanical and acoustical noise inducing a variation of the cavity and refractive index changes by pressure changes of the media inside the FPI, which may all cause intensity variations of the transmitted beam.

Optics EXPRESS

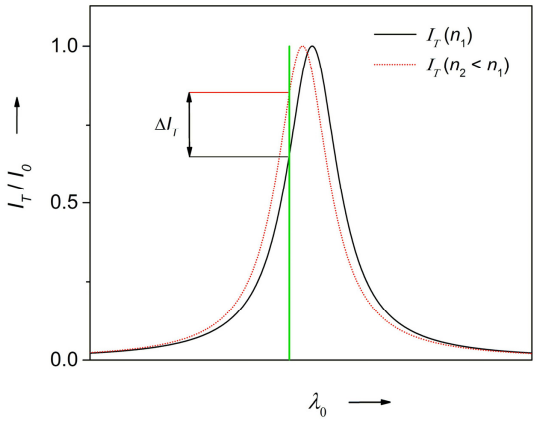

Fig. 1. Operation principle of the FP-FTI. The frequency of a probe laser is tuned near to the inflection point of the periodic transmission function of the interferometer incorporating sample gas at thermal equilibrium (black trace). After a photo-induced heating of the sample by an excitation laser the refractive index of the gas decreases, which is accompanied by a shift of the transmission function with respect to the vacuum wavelength (red dotted trace). This shift is monitored by a change of the transmitted probe laser intensity.

2.2 Sensor system architecture

The layout of the FP-PTI based gas sensor is schematically depicted in Fig. 2. The FPI used as transducer for monitoring induced refractive index changes consisted of two dielectric coated fused silica mirrors with a reflectivity of R = 0.85, a diameter of 12.7 mm, and a radius of curvature of 0.5 m. According to Eq. (3) a finesse of 19.3 can be calculated for this optical cavity. Refractive index changes inside the FPI were monitored by the use of a fiber-coupled, single-mode tunable CW-DFB-LD housed in a butterfly-type 14 pin package (probe laser). The LD emitted at a wavelength around 1600 nm with a minimum optical fiber output power of 20 mW, which was collimated with a fixed-focus aspheric lens collimator. Tuning of the LD could be performed either by the laser chip temperature controlled by a thermoelectric cooler (TEC) or by the injection current controlled by a laser driver. The output beam was coupled by a CaF_2 plano-convex lens (f = 150 mm) into the FPI, whereas the transmitted intensity was detected by a gallium indium arsenide (GaInAs) positive intrinsic negative junction (PIN) photodiode employing a custom made ultra-low noise transimpedance amplifier (TIA). Heating of the sample gas inside the FPI was performed by the use of a collimated CW-DFB-QCL emitting at 7.25 µm (excitation laser), housed in a high heat load package. Here as well, frequency tuning could be performed by QCL temperature and injection current, respectively. The QCL output beam was focused by a plano-convex CaF_2 lens (f = 40 mm) in between the two mirrors forming the FPI, intersecting the standing wave of the probe laser in transverse direction. The two dielectric coated mirrors were fixed to a compact aluminum gas cell with a distance of d = 1 mm to each other. The transmission of the QCL beam through the cell onto a beam dump was enabled by CaF_2 windows also fixed to the cell. Sample gas exchange could be performed by a gas in- and outlet. Figure 3 shows an illustration of the compact and gastight FP-PTI cell designed and used in this work. The outer dimensions of the cell were 40 × 15 × 25 mm, whereas the sample gas volume inside was < 0.7 cm^3. If desired, this value can be easily reduced towards much smaller values down to a few mm^3 by usage of mirrors with smaller diameter, as well as a through hole with lower diameter for QCL beam propagation and closer mirror spacing. The lasers were employed in transverse direction, due to the simple alignment, as well as to avoid heating of the interferometer mirrors, which may alter the optical pathlength of the

Optics EXPRESS

cavity. The sensor platform is based on photothermal sample excitation via WM and second harmonic (2*f*) detection of the transmitted probe beam intensity through the FPI. Detection was performed by demodulation of the alternating current (AC) of the photodetector (PD) signal using a lock-in amplifier (LIA). The direct current (DC) component of the PD was used to maintain the probe laser emission frequency onto the inflection point of the FPI transmission function by a slow feedback circuit (mHz).

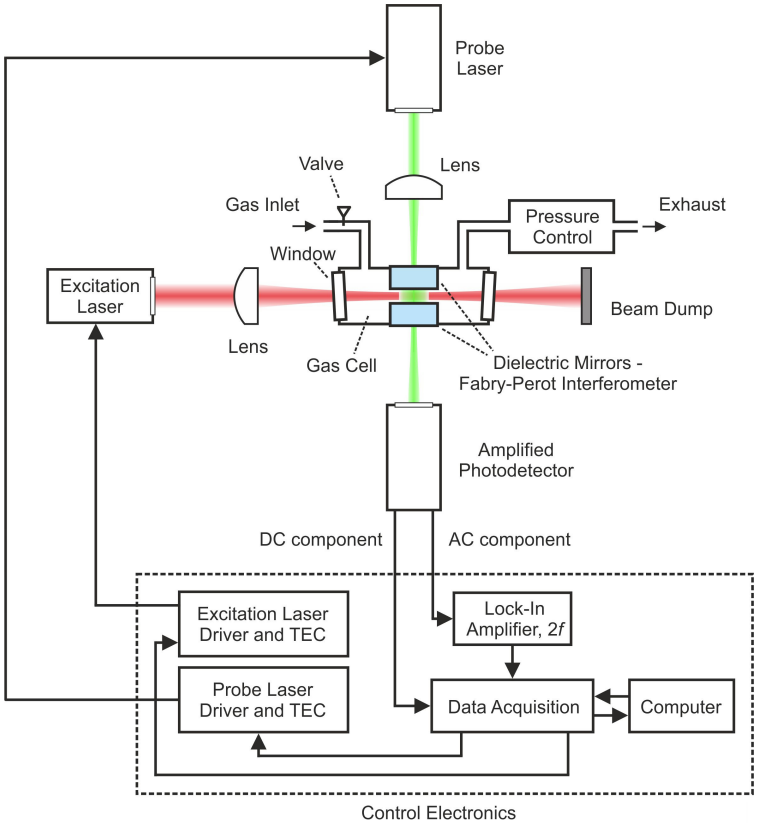

Fig. 2. Schematic of the FP-PTI based gas sensor.

In order to implement the WM technique the emission wavelength of the QCL was modulated with the frequency f_{mod} and modulation depth m by adding a sinusoidal modulation to the DC injection current input. Spectra of the sample gas were acquired by slowly tuning (mHz) the excitation laser frequency over the desired spectral range (from 1380 cm^{-1} to 1379.6 cm^{-1}) through a change of the DC injection current component according to a sawtooth function.

A modulation of the transmitted probe laser intensity, whose frequency was tuned near to the inflection point of one transmission function of the FPI, was induced when the temperature of the sample in between the optical cavity was altered by absorption of excitation laser light. The AC component of the detected photodiode signal was demodulated at second harmonic by a LIA. These signals were digitized by a 24 bit data acquisition card for further data processing, which was carried out with a LabVIEW based program after transferring the digitized data to a computer.

The pressure and flow of the sample gas inside the FP-PTI cell was controlled and maintained by using a metering valve, mini diaphragm vacuum pump, pressure sensor, and pressure controller, all together forming the pressure control.

Optics EXPRESS

The functional principle of the sensor was proved by employing a modulation frequency of f_{mod} = 500 Hz, a modulation depth of m = 0.06 cm^{-1}, a LIA time constant set to τ = 1 second and a sawtooth excitation laser tuning frequency of f = 10 mHz. The absolute pressure and flow of the sample gas was kept constant at p = 200 mbar and v = 110 ml min^{-1}. These parameters were freely chosen for a first performance test of the 2f-WM FP-PTI.

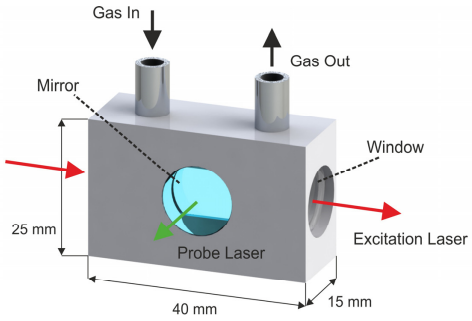

Fig. 3. Illustration of the compact gas cell including the FPI with a mirror spacing of 1 mm.

2.3 Sulfur dioxide absorption band selection

Sulfur dioxide (SO_2) was chosen as target molecule due to strong absorptions in the spectral region of the used QCL. Figure 4 shows a HITRAN simulated spectrum of SO_2 in the spectral region from 6500 to 400 cm^{-1}. Strongest absorption of SO_2 occurs within the range from 1400 to 1300 cm^{-1}, whereas the strongest band is centered around 1348.38 cm^{-1}. This band was not accessible by the employed QCL, therefore a slightly weaker absorption band centered at 1379.78 cm^{-1} was targeted to perform FP-PTI measurements (see insets Fig. 4).

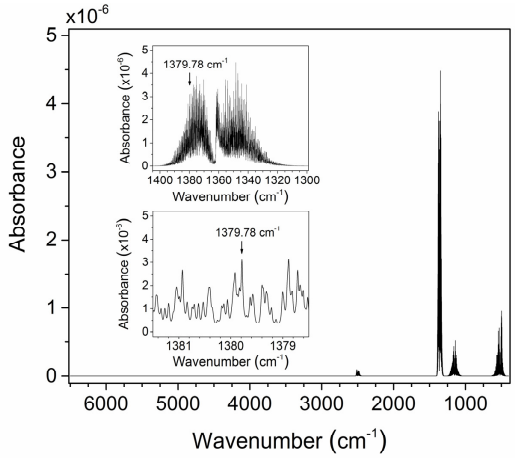

Fig. 4. HITRAN2012 simulated absorption spectrum of 1 ppmv SO_2 (p = 200 mbar, l = 1 cm, T = 296 K) [16].

3. Experimental results

3.1 Sensitivity and linear response of the FP-PTI sensor

In order to verify the functional principle of the presented sensor, spectral scans for different SO_2 concentration levels were performed. For the selected SO_2 absorption band centered at 1379.78 cm^{-1} the measured optical power emitted by the QCL was ~173 mW (T = 288.65 K, I = 416 mA). The QCL beam was focused in between the gap formed by the two

Optics EXPRESS

interferometer mirrors with a transmission efficiency of > 99.9%. Taking the absorption of the plano-convex lens and the optical window of the gas cell into account an optical power of ~150 mW was directed through the two mirrors. The evaluation of the FP-PTI sensors sensitivity and linear response as a function of the SO_2 concentration was investigated by recording spectra within the concentration range from 0 to 1000 parts per million by volume (ppmv) SO_2. Measured results for two different SO_2 concentrations in N_2 together with the noise floor of the sensor when the cell was flushed with pure N_2 are illustrated in Fig. 5(a). The dependence of all measured signal amplitudes versus SO_2 concentrations yielded excellent linearity with a calculated R-square value of 0.9998, shown in Fig. 5(b).

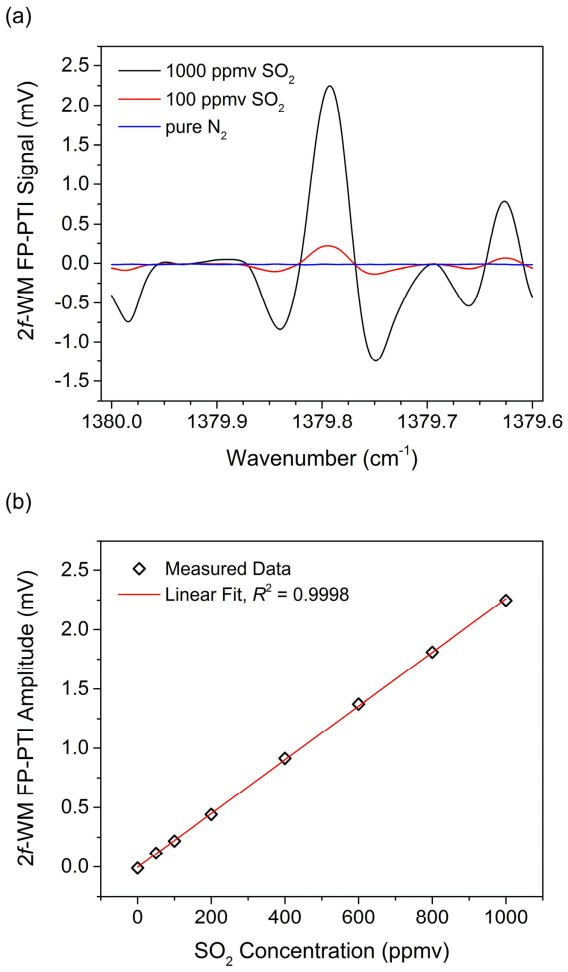

Fig. 5. (a) 2*f*-WM FP-PTI spectra of two different SO_2 concentrations and the sensors noise floor for pure N_2 recorded at an absolute pressure of p = 200 mbar when the QCL frequency was tuned over the absorption band centered at 1379.78 cm^{-1}; (b) Linear sensor response of measured SO_2 signal amplitudes versus gas concentration.

Based on the measured signal amplitude of 100 ppmv SO_2 and the standard deviation of the noise level for pure N_2 a SNR of ~90 was calculated, which yields a 1 σ minimum detection limit (MDL) of 1.1 ppmv for a 1 second acquisition time. The normalized noise equivalent absorption (NNEA) coefficient at unit laser power and at unit bandwidth allows to compare indirect spectroscopic sensors. This coefficient was recalculated to be $NNEA = 1.8 \times 10^{-6}$ cm^{-1} W $Hz^{-1/2}$, using a minimum detectable SO_2 absorption coefficient of $\alpha_{min} = 3.3 \times$

Optics EXPRESS

10^{-6} cm^{-1}, an optical excitation power of P = 150 mW, and a detector bandwidth of Δf = 78 mHz (τ = 1 s, 24 dB/oct low-pass filter).

4. Conclusions and outlook

The presented work illustrates the high potential for further development of the sensitive and selective gas sensor scheme facilitating an ultra-small detection volume. The set-up is based on a compact and robust arrangement without the use of any moveable part. Such a sensor may be of interest for applications either where only small sample gas volumes are available or for detection of fast changing concentration levels in gas streams. Moreover, the setup provides an overall small size, which may be advantageous for certain implementations such as mobile applications. The functional principle of the sensor arrangement was proved by targeting SO_2 in N_2, which yielded a MDL of 1.1 ppmv and a corresponding NNEA of 1.78 × 10^{-6} cm^{-1} W $Hz^{-1/2}$. The value of this NNEA coefficient is a bit worse in respect to that of a comparable laser based SO_2 sensor detecting photoacoustic signals [17]. The difference in sensitivity results from the fact that the SNR of the presented FP-PTI suffers from an increased technical noise level, in contrast to the photoacoustic system. However, the presented work is meant to depict the potential of the 2*f*-WM FP-PTI technique rather than illustrate highest sensitivity. Improvements in terms of sensitivity can be achieved on the one hand by an increase of detectable signal and on the other hand by noise reduction. Signal enhancement may be achieved by diverse measures, such as the use of a FPI with higher finesse, which is simply enabled by employing mirrors with a higher reflectivity. An increase in sensitivity by the finesse, however, can only be achieved to a point where noise is not increased proportionally. Due to the fact that the PTS signal is directly proportional to the excitation laser power and inversely proportional to the excitation volume, this technique will greatly benefit from higher excitation power levels as well as further senor miniaturization. Prominent noise is introduced by probe laser intensity and frequency noise. According to the data sheet the utilized probe laser had a linewidth of 2 MHz. Limiting noise arising from probe laser frequency noise, which translates into intensity noise by transmission through the FPI can greatly be improved by employing lasers with a narrower linewidth and an adequate driver. Also optical feedback arising from unintended reflections of the emitted light back into the laser cavity may introduce additional laser noise. Such reflections may occur e.g. at the FPI. A higher optical isolation as the integrated 30 dB isolator will minimize these back reflections more efficiently. Improvements referring to environmental noise such as mechanical vibrations and acoustic waves, which may introduce spacing variations or a misalignment of the mirrors, can be achieved by an efficient shield which surrounds the interferometer, or by employing any reference. Such a countermeasure may also minimize changes in the refractive index of the sample gas being directly caused by sound. The effect that pressure waves also cause a change in refractive index is exploited by optical microphones using an interferometer to detect sound [18,19]. Due to the lack of any resonance the modulation (detection) frequency can be freely selected. By the use of higher modulation frequencies the 1/*f* noise can be improved. However, the generated signal decreases proportionally since the photo-induced temperature change is inversely proportional to the modulation frequency. An optimization study in terms of modulation frequency will improve the sensor performance. Furthermore, the heat production rate is dependent on the energy transfer from vibrational to translational degrees of freedom (V-T relaxation) of the target gas [20]. If the V-T relaxation is fast compared to the modulation frequency, the heat production is independent of the molecular relaxation. But if the relaxation is slow compared to the modulation frequency the heat production is suppressed. By this means a slow V-T relaxation or fast modulation can strongly influence the heat production. The V-T relaxation rate is decreased at reduced pressure, which may lead suppressed signals employing modulation frequencies above ~10 kHz. Moreover, the WM technique enables the optional use of an excitation laser reference channel, which may

Optics EXPRESS

consist of a reference cell and a photodetector signal demodulated at 3*f*. By this means the excitation laser frequency can be locked to the center of the selected absorption line in order to avoid any laser-drifts. This static mode of WM operation can be used to increase sample quantification rate, as in the case of PTS methods typical LIA constants of 100 to a few 100 ms are used. Therefore, spectral scans may take a few seconds to minutes, in contrast to single point quantification. In case of slowly changing concentration levels an optimum average time can be found for a further increase in sensitivity. Finally, an optimization study of the within this work freely chosen parameters (pressure, modulation frequency, modulation depth, LIA time constant) will yield an improved sensor SNR.

Funding

Austrian research funding association FFG under the scope of the COMET program (contract #843546). Carinthian Tech Research. Open access funding program of the TU Wien University Library.